Article

DNA probes for implementation of multiple molecular computations using a lateral flow strip biosensor as the sensing platform

Junhua Chen, Shu Chen, and Fengling Li

Anal. Chem., **Just Accepted Manuscript** • DOI: 10.1021/acs.analchem.8b02103 • Publication Date (Web): 03 Aug 2018

DNA probes for implementation of multiple molecular computations using a lateral flow strip biosensor as the sensing platform

Junhua Chen,* Shu Chen, and Fengling Li

Guangdong Key Laboratory of Integrated Agro-environmental Pollution Control and Management, Guangdong Institute of Eco-environmental Science & Technology, Guangzhou 510650, China

*Corresponding author:

E-mail: 222chenjunhua@163.com

Abstract

A series of advanced logic circuits have been successfully constructed to perform multiple arithmetic functions using a lateral flow strip biosensor as the sensing platform, including half adder, half subtractor, multiplexer, demultiplexer, and keypad lock. In each circuit computing, the computing elements are the DNA probes, which can implement the DNA assembly process to generate the output single-stranded nucleic acid. The strip biosensor is used as the sensing platform to distinguish the output of the logic gates. The distinctive advantage of our proposed biocomputing system is that the logic events can be transformed into the red bands on the test zones, which can be observed by the naked eye. The logic system with convenient operation, rapid response, and cost-effectiveness features will facilitate the portable analysis at ambient temperature without resorting to any instrumentation. The versatility and power of the logic computation demonstrated here indicate its great potential in intelligent point-of-care (POC) disease diagnosis and on-site environmental monitoring.

Introduction

Molecular logic devices, which can be viewed as molecular-scale computers that possess the ability to combine multiple logic circuits to perform binary arithmetic processing, hold great promise for disease diagnostics, intelligent biosensing, and biomarker detection.[1-8] In recent years, considerable efforts have been made to fabricate a variety of logic gates, including AND, OR, XOR, NOR, INHIBIT and so on.[9-12] Most of the reported molecular logic gates employ fluorescent or electrochemical signals as the outputs, which relies on advanced instruments for the readout and lacks the desired portability.[13-16] In recent years, lateral flow strip biosensors have attracted considerable attention because of their outstanding characteristics, such as simple operation, short assay time, user-friendly format, and cost-effectiveness, which make them particularly suitable for on-site applications.[17,18] Using gold nanoparticles as the signal reporter, the output of the strip can be readily distinguished by the naked eye. Furthermore, the strip biosensor minimizes the requirements of professional operators and eliminates multiple analysis steps involving sophisticated instruments. The qualitative results can be determined visually by observing the color intensity of the red band on the test zone, and the quantitative data can be obtained by recording the colorimetric responses by a handheld "strip reader", making the readout and analysis of the results a rapid and efficient process. Our group and others have pioneered the use of strip biosensors for the detection of nucleic acids,[19,20] proteins,[21,22] and heavy metal ions.[23,24] To date, different computing paradigms with the strip sensing platform were focused on the fabrication of elementary logic gates.[25-29] However, advanced logic circuits are rarely achieved at the strip biosensors due to the increased computational complexity of the process, which requires the integration of individual logic gates into larger circuits to execute sophisticated algorithms. Although complex high-level logic circuits are critical for data calculating and processing,[30-32] the construction of these circuits at the molecular level is still a great challenge, especially in strip operations. To make further advancements in molecular computation, we constructed a

series of advanced logic circuits using the strip as the sensing platform to emulate the multi-channel capabilities of the processors, including half adder, half subtractor, multiplexer, demultiplexer, and keypad lock. These strip networks are endowed with portability, short assay time, naked-eye readout, long-term stability, and cost-effectiveness. We expect that our present logic system on a simple and universal computing platform will find great potential in point-of-care (POC) applications for intelligent disease diagnosis and environmental monitoring.

Experimental Section

Materials: $HAuCl_4 \cdot 3H_2O$, trisodium citrate, Triton X-100, $MgCl_2$, bovine serum albumin (BSA), and tris-(hydroxymethyl)aminomethane (Tris) were purchased from Sigma-Aldrich (St. Louis, Mo). Streptavidin-coated magnetic beads (2.8 μM in diameter) were purchased from Life Technologies (Grand Island, NY). Other reagents and chemicals were of analytical grade and used without purification. All solution was prepared with ultrapure water (18.2 MΩ/cm) from a Millipore Milli-Q water purification system (Billerica, MA).

All DNA sequences were designed to minimize undesired cross-hybridization using NUPACK (http://www. nupack.org/). DNA oligonucleotides were HPLC-purified and purchased from Shanghai Sangon Biotechnology Co., Ltd. (Shanghai, China) and their sequences were listed in the Supporting Information.

Preparation of the strip platform: The logic strip is made up of four components: sample pad, conjugate pad, nitrocellulose membrane, and absorption pad. The sample pad was made from glass fiber and treated with 20 mM Tris-HCl buffer (pH 8.0, 0.25% Triton X-100, 150 mM NaCl). The protocols for preparing gold nanoparticles (AuNPs) and AuNPs-DNA conjugates were described in the Supporting Information. The conjugate pad was prepared by dispensing 5 μL of AuNPs-DNA conjugate solution onto the glass fiber using the dispenser HM3030

(Shanghai Kinbio Tech. Co., Ltd. Shanghai, China). The test zone and control zone were prepared by dispensing respective test probe (30 μL, 100 μM) and control probe (30 μL, 100 μM) on the nitrocellulose membrane. The membrane was then exposed under the UV lamp for 8 min to facilitate the immobilization of those DNA probes. Finally, the sample pad, conjugate pad, nitrocellulose membrane, and absorption pad were assembled on a plastic adhesive backing (60 mm x 30 cm), and each part overlapped 2 mm to ensure migration of the solution through the strip during the assay. Strips with a 4 mm width were cut by using a programmable strip cutter ZQ2000 (Shanghai Kinbio Tech. Co., Ltd. Shanghai, China).

*Logic circuit operation:*All reactions were performed in 20 mM Tris-HCl buffer (pH 7.4, 200 mM NaCl, 20 mM $MgCl_2$) at a final DNA concentration of 1 μM. The samples, without the inputs, were heated to 90 ^{o}C for 10 min, and then cooled down to room temperature for 90 min. The input was added to the above solution, and the mixture was incubated for 120 min at room temperature. The mixed sample solution (total volume, 50 μL) was applied to the sample pad of the strip for assay. Accumulation of AuNPs on the test and control zones generated characteristic red bands. The red bands were visualized within 10 min. The red bands were observed both on the test and control zones to indicate a "true" result (output = 1), while only one red band was observed on the control zone to indicate a "false" result (output = 0). The images were recorded with a digital camera. The intensities of the red bands on the test and control zones were recorded by using the portable “strip reader” equipped with the “GoldBio strip reader” software (Shanghai Kinbio Tech. Co., Ltd. Shanghai, China), which could search the red bands in a fixed reaction area automatically and then calculate parameters such as peak height and area integral.

Results and Discussion

Half adder

The Mg^{2+}-dependent DNAzyme[3,33,34] was split into two fragments and employed as the functional units for the construction of the logic systems. The "computing elements" is the DNA probes (DNA1-10). In the present of appropriate input, the split subunits may assemble into active DNAzyme structures *via* input-induced cooperative association of the split fragments, leading to the cleavage of a ribonucleobase (rA)-containing DNA substrate. Figure 1 illustrates the principle of the half adder operation. A half adder can perform a binary addition by integration of an XOR gate and an AND gate in parallel to generate a SUM (S) output and a CARRY (C) output, respectively.[35,36] In the absence of any input (0,0), the logic system doesn't work and no active DNAzyme is formed. The nucleic acid segements m-n and p-q are in a caged state. Thus, no red band is produced in the test zones and the output is 0. The red bands on the control zones of the strips can be observed in all input combinations, indicating that the logic strip biosensor is working properly. In the presence of either input1 or input2 (1,0 or 0,1), two different DNAzyme structures are formed *via* input-mediated cooperative conjunction of respective DNAzyme subunits (DNA (1)/(2) for input1 and (3)/(4) for input2), leading to the cleavage of the mutual caged substrate (7)/(8) and to the release of the protected sequence m-n. The liberated single-stranded nucleic acid m-n can be defined as the output1, which encodes the XOR gate. The strip biosensor is used as the sensing platform to distinguish the output of the logic gate.The nucleic acid m-n then is applied on the sample pad of the strip. The solution migrates by capillary action, passes the conjugate pad, and then rehydrates the gold nanoparticles (AuNPs)-m*-p* probe conjugate. The domain m of the released DNA hybridizes with the segment m* to form the complex (AuNPs-m*/m-p) and continue to migrate along the strip. The hybrids are captured on the test zone 1 (TZ1) by the second hybridization between domain n of the released DNA and the immobilized DNA n*. The accumulation of AuNPs on TZ1 is visualized as a characteristic red band and the output

reads 1, representing an XOR gate. The excess of AuNPs-m*-p* conjugates continue to migrate and are captures on the control zone (CZ) by the complementary hybridization between m*-p* and m-p, thus generating a secongd red band. In the presence of both inputs (1,1), the energetically favored duplex between input1 and input2 will be formed. This prohibits the formation of the active DNAyzme from the subunits (1)-(4) and the generation of red band on TZ1. However, the hybridization events between the two inputs can draw the segments e and f together and facilitate the formation of another synergistically-stabilized catalytic DNAzyme from (5)/(6) subunits. Then, the released DNA p-q after cleavage reaction can be defined as the output2, which encodes the AND gate. The nucleic acid p-q then is applied on the sample pad of the strip and can be captured on TZ2 to give a red band to indicate an AND gate operation. Figure 2A presents typical photo images of the half adder, and Figure 2B and C show the corresponding results. In such a combinational circuit, the XOR and the AND gates are implemented in parallel and are triggered by the same inputs, fitting the requirements for a half adder. The truth table and circuitry are given in Figure 2D and E, respectively.

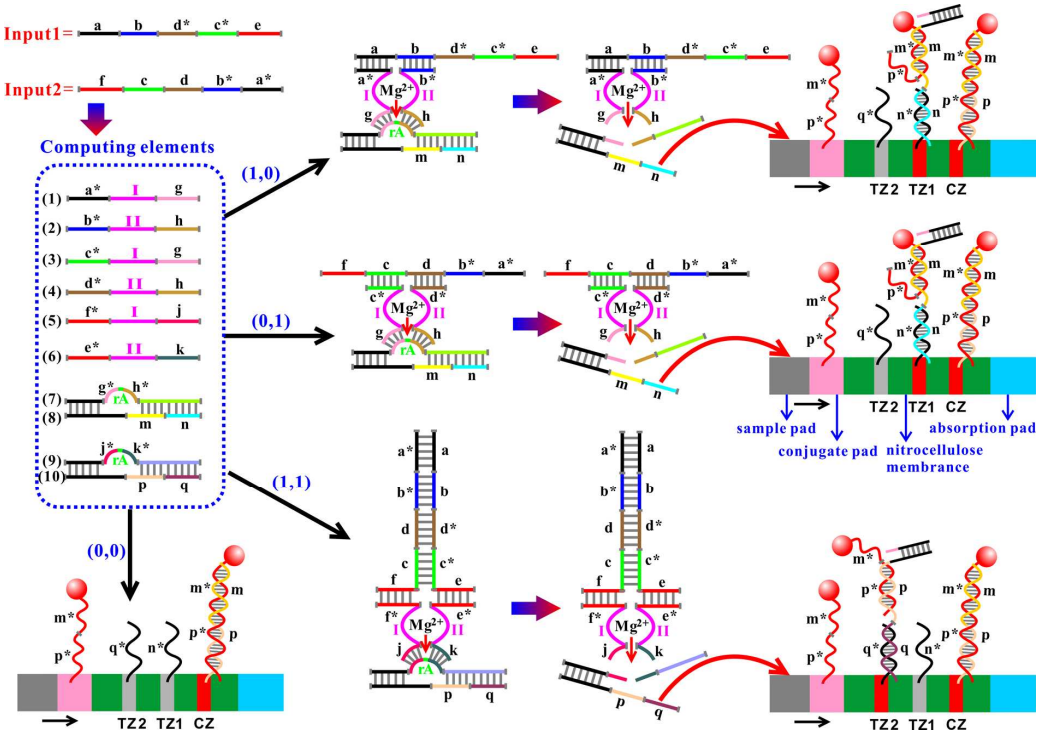

Figure 1. Schematic illustration of half adder operation. The split Mg^{2+}-dependent DNAzyme subunits (1)-(6) and the substrate DNA (7)/(8) and (9)/(10) are used as the computing elements to construct the circuit. Domains I and II are the catalytic core components of the DNAzyme. A starred domain denotes a domain complementary in sequence to the domain without a star. The strip consists of four components: sample pad, conjugate pad, nitrocellulose membrane, and absorption pad. Using gold nanoparticles as the indicator, the output can be directly visualized by the naked eye. CZ, the control zone; TZ1, the test zone 1; TZ2, the test zone 2.

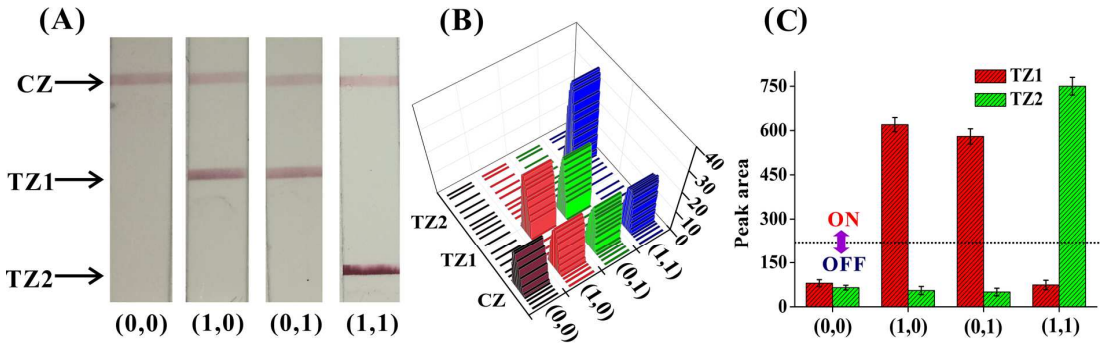

(D)

Inputs		Output1 (TZ1)	Output2 (TZ2)
Input1	Input2	XOR gate Sum Digit	AND gate Carry Digit
0	0	0	0
1	0	1	0
0	1	1	0
1	1	0	1

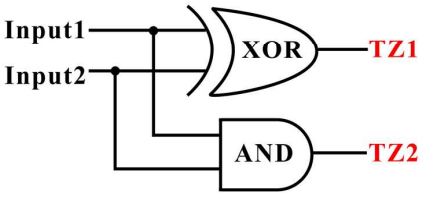

Figure 2. (A) Photographs of the strips in the half adder operation. (B) Their corresponding optical response results. (C) Column diagram of the peak areas of the red bands on TZ1 and TZ2. The red dashed line marks the threshold value of 220. (D) Truth table depicting the half adder. (E) Diagram of the electronic half adder logic circuit.

Half subtractor

A half subtractor was also constructed based on the same strip platform and two new designed inputs. Figure 3 depicts the construction of the half subtractor. The "computing elements" is the DNA probes (DNA1-10). A half subtractor requires the parallel activation of an XOR gate and an INHIBIT gate to produce a DIFFERENCE (D) output and a BORROW (B) output, respectively.[37,38] It should be noted that an XOR gate is realized in a half subtractor just as the same in a half adder, yielding a red band on TZ1 in the presence of either input. The XOR gate in the half subtractor provides the DIFFERENCE digit. Meanwhile, an INHIBIT gate is implemented using the liberated single-stranded nucleic acid p-q as the output, which can be caputured on TZ2 and gives the red band on TZ2. In the presence of input1, the protected sequence p-q is still occupied, failing to generate free p-q segement. In the presence of input2, an active DNAzyme from the subunits (5)/(6) is formed, releasing the caged nucleic acid p-q after the cleavage of the caged substrate (9)/(10). When the two inputs coexist, the input1 and input2 hybridize together, inhibiting the formation of any active DNAzyme. Thus the sequence p-q is still protected and the output reads 0. The INHIBIT gate in the half subtractor yields the BORROW digit. Figure 4A presents typical photo images of the half subtractor, and Figure 4B and C show the corresponding results. The half subtractor is successfully achieved by integrating the XOR gate and the INHIBIT gate simultaneously. The truth table and circuitry are given in Figure 4D and E, respectively.

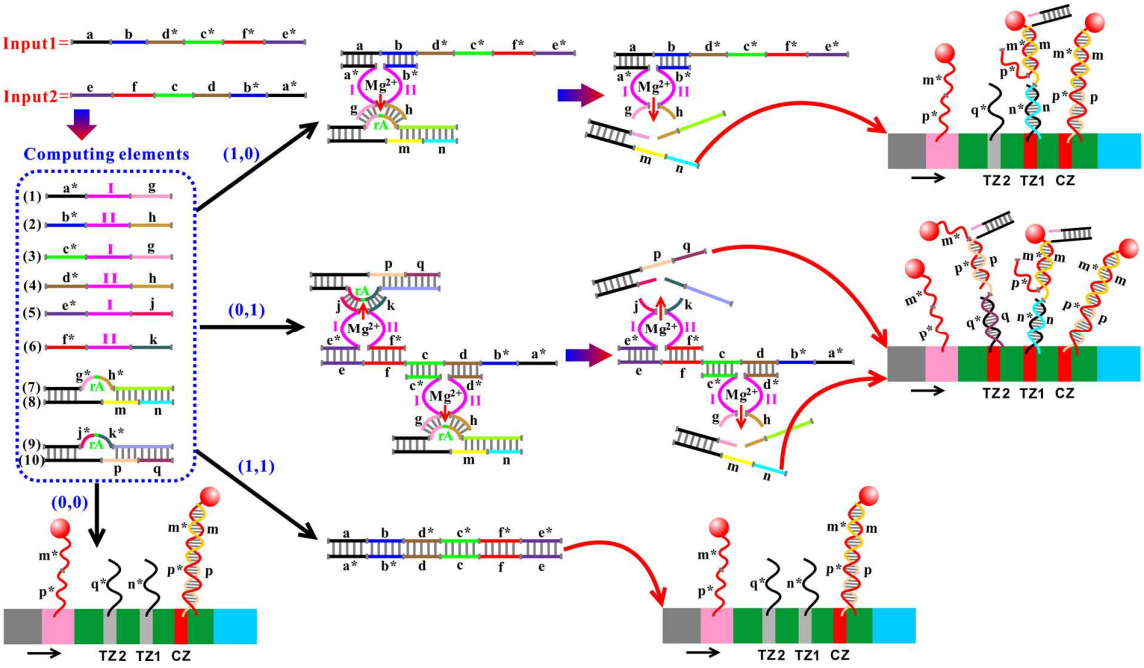

Figure 3. Schematic illustration of half subtractor operation. The split Mg^{2+}-dependent DNAzyme subunits (1)-(6) and the substrate DNA (7)/(8) and (9)/(10) are used as the computing elements to construct the circuit. The red band on TZ1 encodes the XOR gate and the red band on TZ2 encodes the INHIBIT gate.

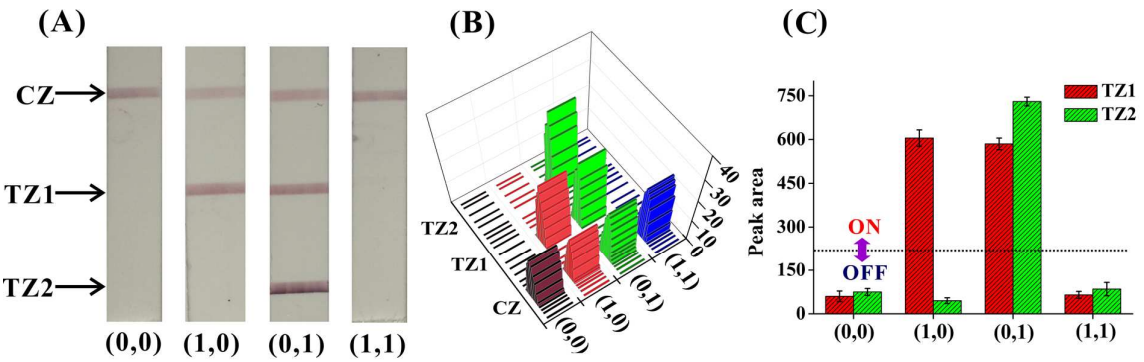

(D)

Inputs		Output1 (TZ1)	Output2 (TZ2)
Input1	Input2	XOR gate Difference Digit	INHIBIT gate Borrow Digit
0	0	0	0
1	0	1	0
0	1	1	1
1	1	0	0

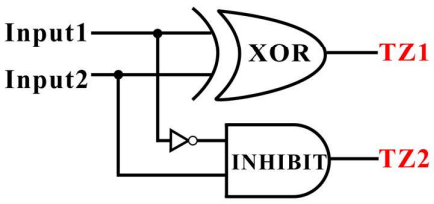

Figure 4. (A) Photographs of the half subtractor operation. (B) Their corresponding optical response results. (C) Column diagram of the peak areas of the red bands on TZ1 and TZ2. The red dashed line marks the threshold value of 220. (D) Truth table depicting the half subtractor. (E) Diagram of the electronic half subtractor logic circuit.

2:1 multiplexer

To achieve higher complexity of the biocomputing system for information processing using the simple and visual strip sensing platform, we further fabricated a 2:1 multiplexer. The 2:1 multiplexer can transform two different inputs into a single output channel with the help of one selector, thus mimicking data compression.[39,40] Figure 5 outlines the implementation principle of the 2:1 multiplexer. The "computing elements" is the DNA probes (DNA1-6). In the presence of input1 (1,0) or both inputs (1,1) without the selector, the assembly of an active DNAzyme from the subunits (1)/(2) is realized, resulting in the cleavage of the caged substrate (5)/(6) and generating the uncaged sequence p-q as the output,

which can be captured on TZ1 to give a red band. In the presence of the selector, the treatment of the system with input1 (1,0) prohibits the assembly of the subunits (1)/(2) due to the energetically preferred hybridization between input1 and the selector. In the presence of input2 (0, 1) or both inputs (1,1) with the selector, the cooperatively stabilized DNAzyme is formed *via* the input/selector-guided assembly of the subunits (3)/(4). This leads to the cleavage of the caged substrate (5)/(6) and generating free sequence p-q as the output, which can be captured on TZ1 to give a red band. The subunits (1)/(2) and (3)/(4) have the same regions j and k, hence, the two DNAzyme structures share the substrate (5)/(6). Figure S1A and D (Supporting Information) present typical photo images of the 2:1 multiplexer, and Figure S1B, C, E and F show the corresponding results. The system would transmit input1 into the output channel in the absence of the selector and transmit input2 into the output channel in the presence of the selector, thus confirming that the logic strip functions as a 2:1 multiplexer. The truth table and circuitry are given in Figure S1G and H, respectively.

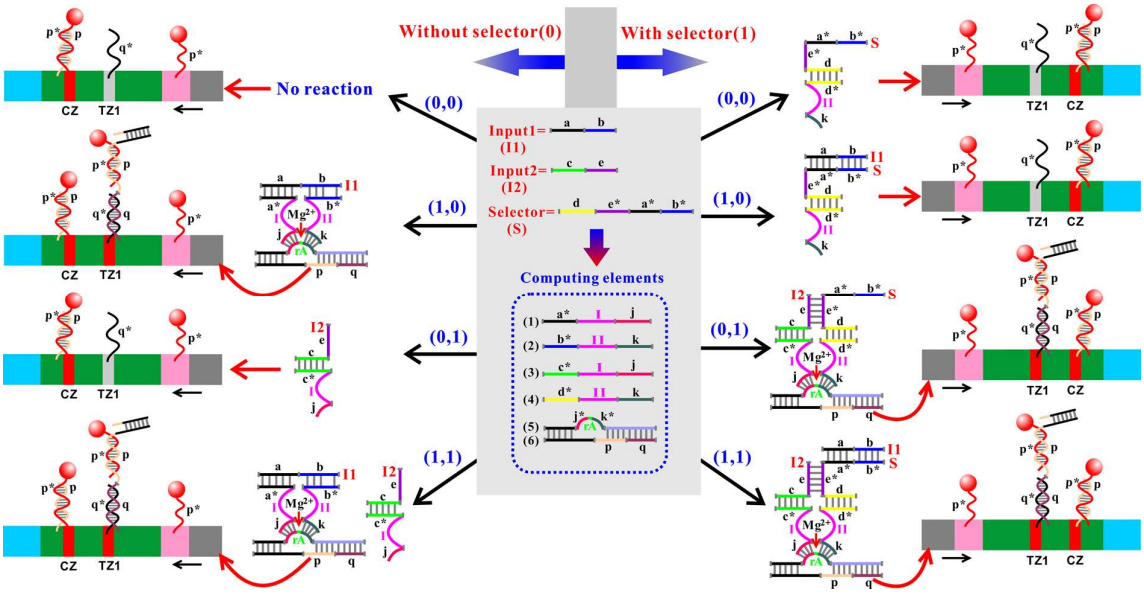

Figure 5. Schematic illustration of the strip 2:1 multiplexer operation. The split Mg^{2+}-dependent DNAzyme subunits (1)-(4) and the substrate DNA (5)/(6) are used as the computing elements to construct the system in the absence/presence of the selector. I1, the input1; I2, the input2; S, the selector.

1:2 demultiplexer

The split DNAzyme subunits were also employed to construct a 1:2 demultiplexer, which plays an opposite function to a 2:1 multiplexer in that it can transmit one input signal into two output channels with the help of a selector, thus mimicking data decompression.[41,42] Figure 6 illustrates the implementation principle of the 1:2 demultiplexer. The "computing elements" is the DNA probes (DNA1-7). In the absence of selector and input1 (0,0), the sequence m-n is occupied and no red band on TZ is observed due to the lack of formation of an active DNAzyme. Similarly, in the presence of selector and the absence of input1 (1,0), the sequence p-q is occupied and no red band on TZ is observed since no catalytic DNAzyme is formed. In the absence of selector and the presence of input1 (0,1), an active DNAzyme from the subunits (1)/(2) is formed. After the cleavage of the caged substrate (4)/(5), the available DNA m-n (output1) can be captured on TZ1 and gives a red band on TZ1. In the coexistence of selector and input1 (1,1), another active DNAzyme from the subunits (1)/(3) is formed, leading to the catalytic cleavage of the caged substrate (6)/(7) and the generation of the free DNA p-q as the output2. Figure S2A (Supporting Information) presents typical photo images of the 1:2 demultiplexer, and Figure S2B and C show the corresponding results. The system would transmit input1 into the output channel 1 (red band on TZ1) in the absence of the selector and transmit input1 into the output channel 2 (red band on TZ2) in the presence of the selector, thus confirming that the logic strip functions as a 1:2 demultiplexer. The truth table and circuitry are given in Figure S2D and E, respectively.

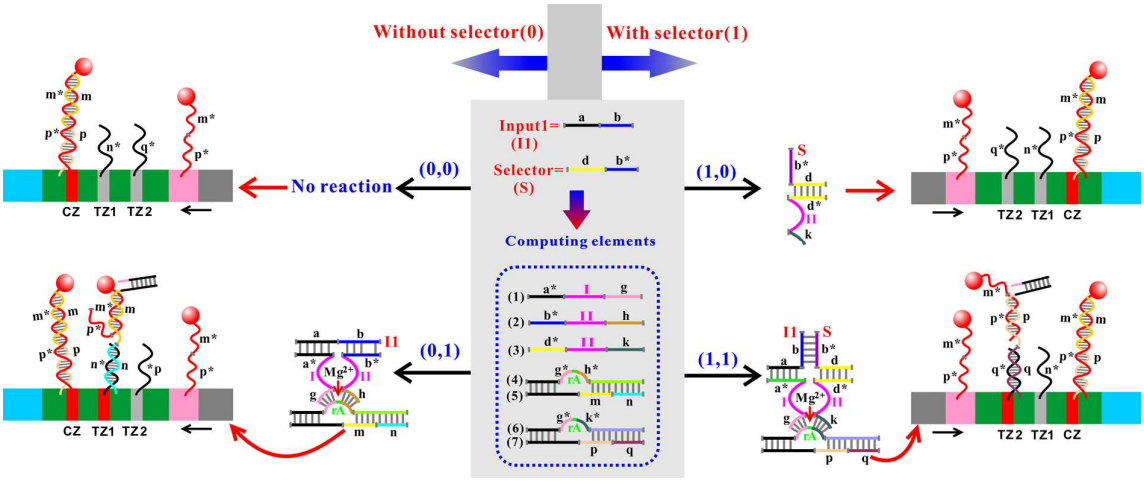

Figure 6. Schematic illustration of 1:2 demultiplexer operation. The split Mg^{2+}-dependent DNAzyme subunits (1)-(3) and the substrate DNA (4)/(5) and (6)/(7) are used as the computing elements to construct the system in the absence/presence of the selector.

Keypad lock

To demonstrate the scalability of the biocomputing and the communication between different logic gates, we have designed multilayer circuits that work as a keypad lock security system. The keypad lock represents a new approach for protecting information at the molecular level. The output of a keypad lock not only depends on the proper combination of the inputs but also on the correct order by which the inputs are introduced.[10,43,44] To open this lock, one needs to know the exact password. Figure 7 illustrates the mode of operation of the serial gates working as a keypad lock. The "computing elements" is the DNA probes (DNA1-12). The three input signals are conjugated with magnetic beads. Rinsing of the magnetic beads after each hybridization reaction can eliminate the wrong DNA inputs. In the presence of input1 (A), the first active DNAzyme is generated from the subunits (1)/(2), leading to the cleavage of the caged substrate (7)/(8). The released DNA m-n then acts as the input for the next gate. In the presence of input2 (B), the second active DNAzyme corresponding to the subunits (3)/(4) is formed, resulting in the cleavage of the caged substrate (9)/(10). The

unprotected DNA u-v together with the input3 (C) activate the third DNAzyme from the subunits (5)/(6) to cleave the caged substrate (11)/(12). After magnetic separation, the liberated DNA p-q served as the output will be left in solution and can be captured on TZ1 and gives a red band on TZ1. The final results of the keypad lock can be easily distinguished by the naked eye. Only one correct order of the three input signals (ABC) generates the free DNA p-q that opens this lock. Other input permutations (ACB, BAC, BCA, CAB, and CBA) fail to open this lock and no red band on TZ1 is observed. Furthermore, by appropriately tailoring of the substrate (11), we can design an ultrasensitive biosensor for input1 assay. The "waste" DNA (the sequence is the same as the input1) after the cleavage of the caged substrate (11) can be used as the trigger to activate the feedback mechanism that amplifies and enriches the output signal in a cascaded manner. Figure 8A presents typical photo images of the keypad lock, and Figure 8B and C show the corresponding results. This lock is opened only when the inputs are introduced in an exact order (ABC). A truth table is given in Figure 8D.

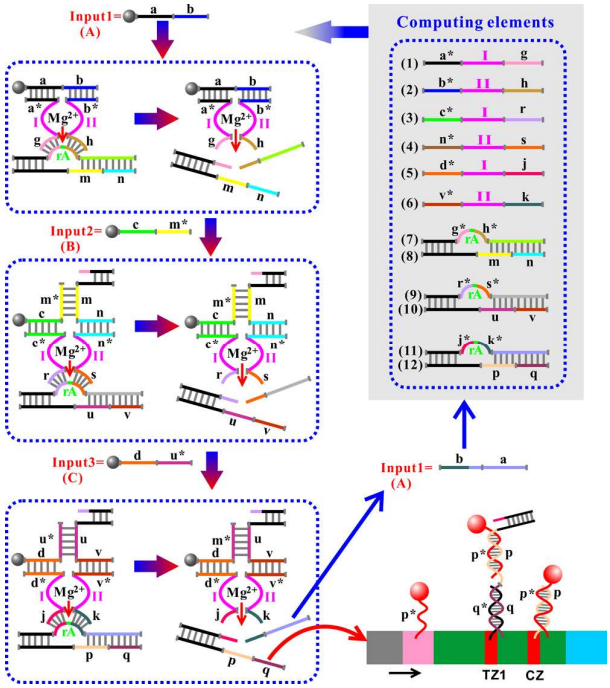

Figure 7. Schematic illustration of keypad lock operation. The split Mg^{2+}-dependent DNAzyme subunits (1)-(6) and the substrate DNA (7)/(8), (9)/(10), and (11)/(12) are used as the computing elements to construct the cascaded gates. The three input signals (A, B, and C) are conjugated with magnetic beads.

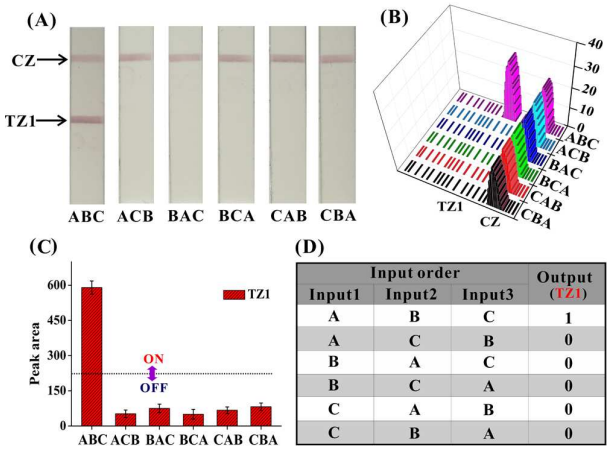

Input order			Output (TZ1)
Input1	Input2	Input3	
A	B	C	1
A	C	B	0
B	A	C	0
B	C	A	0
C	A	B	0
C	B	A	0

Figure 8. (A) Photographs of the strips in the keypad lock operation. (B) Their corresponding optical response results. (C) Column diagram of the peak areas of the red bands on TZ1 and TZ2. The red dashed line marks the threshold value of 220. (D) Truth table depicting the keypad lock.

Conclusion

In summary, several advanced logic circuits (half adder, half subtractor, multiplexer, demultiplexer, and keypad lock) have been successfully demonstrated to perform multiple arithmetic functions in proof-of-principle using AuPNs as the indicators and the lateral flow strip biosensor as the sensing platform. In each arithmetic circuit, the DNA probes (computing elements) implement the logic computation function to generate the output (single-stranded nucleic acid). In the present of appropriate input, the split DNAzyme subunits assemble into active configurations *via* input-induced cooperative conjunction of the split fragments, leading

to cleavage of the caged substrate. The strip biosensor is used as the sensing platform to recognize the released single-stranded DNA (output) from the caged substrate. In comparison with previously reported fluorescent or electrochemical logic gates, this is the first use of a strip as the sensing platform to construct high-order logic circuits with enhanced computational complexity. The distinctive advantage of our proposed biocomputing system is that the logic events can be transformed into the red bands on the test zones, which can be unambiguously read out by the naked eye. Moreover, the strip with the features of simplicity, cost-effectiveness, portability, and convenience will be a promising molecular platform to emulate the multi-channel capabilities of the cascaded logic networks. The scalability and versatility of molecular computing based on strips here indicate their promising applications in the fabrication of intelligent devices and logic biosensors for POC disease diagnosis and in-field environmental monitoring.

ASSOCIATED CONTENT

Supporting Information

The DNA sequences, the protocols for preparation of gold nanoparticles and gold-DNA conjugates, and figures S1 and S2 were listed in the Supporting Information.

The Supporting Information is available free of charge on the ACS Publications website.

AUTHOR INFORMATION

Corresponding Author:

*E-mail: 222chenjunhua@163.com

Notes

The authors declare no competing financial interest.

ACKNOWLEDGMENT

Financial support was provided by the GDAS' Special Project of Science and Technology Development (2017GDASCX-0405), the Guangdong Natural Science Funds for distinguished Young Scholar (2016A030306012), the Special Support Program for Young Talent Scholar of Guangdong Province (2015TQ01Z092), the Local Innovative and Research Teams Project of Guangdong Pearl River Talents Program (2017BT01Z176), and the SPICC Program (2016GDASPT-0105).

References

(1) Mailloux, S.; Gerasimova, Y. V.; Guz, N.; Kolpashchikov, D. M.; Katz, E. *Angew. Chem. Int. Ed.* **2015**, *54*, 6562-6566.

(2) Wang, S.; Sun, J.; Zhao, J.; Lu, S.; Yang, X. *Anal. Chem.* **2018**, *90*, 3437-3442.

(3) Chen, J.; Pan, J.; Chen, S. *Chem. Sci.* **2018**, *9*, 300-306.

(4) Huang, W.; Zhou, Y.; Du, J.; Deng, Y.; He, Y. *Anal. Chem.* **2018**, *90*, 2384-2388.

(5) Hou, T.; Zhao, T.; Li, W.; Li, F.; Gai, P. *J. Mater. Chem. B* **2017**, *5*, 4607-4613.

(6) Li, Y.; Li, W.; He, K.; Li, P.; Huang, Y.; Nie, Z.; Yao, S. *Nanoscale* **2016**, *8*, 8591-8599.

(7) Zhang, C.; Yang, J.; Jiang, S.; Liu, Y.; Yan, H. *Nano. Lett.* **2016**, *16*, 736-741.

(8) Lin, X.; Liu, Y.; Deng, J.; Lyu, Y.; Qian, P.; Li, Y.; Wang, S. *Chem. Sci.* **2018**, *9*, 1774-1781.

(9) Gerasimova, Y. V.; Kolpashchikov, D. M. *Angew. Chem. Int. Ed.* **2016**, *55*, 10244-10247.

(10) Chen, J.; Zhou, S.; Wen, J. *Angew. Chem. Int. Ed.* **2015**, *54*, 446-450.

(11) Maranhao, A. C.; Ellington, A. D. *Nature Biotechnol.* **2013**, *31*, 413-415.

(12) Yu, S.; Wang, Y.; Jiang, L.; Bi, S.; Zhu, J. *Anal. Chem.* **2018**, *90*, 4544-4551.

(13) Ge, L.; Wang, W.; Sun, X.; Sun, T.; Li, F. *Anal. Chem.* **2016**, *88*, 9691-9698.

(14) Wang, W.; Huang, S.; Li, J.; Rui, K.; Bi, S.; Zhang, J.; Zhu, J. *Chem. Sci.* **2017**, *8*, 174-180.

(15) Bi, S.; Yue, S.; Wu, Q.; Ye, J. *Chem. Commun.* **2016**, *52*, 5455-5458.

(16) Chen, J.; Zeng, L. *Biosens. Bioelectron.* **2013**, *42*, 93-99.

(17) Yang, M.; Zhang, W.; Yang, J.; Hu, B.; Cao, F.; Zheng, W.; Chen, Y.; Jiang, X. *Sci. Adv.* **2017**, *3*, eaao4862.

(18) You, M.; Lin, M.; Gong, Y.; Wang, S.; Li, A.; Ji, L.; Zhao, H.; Ling, K.; Wen, T.; Huang, Y.; Gao, D.; Ma, Q.; Wang, T.; Ma, A.; Li, X.; Xu, F. *ACS Nano* **2017**, *11*, 6261-6270.

(19) Du, Y.; Pothukuchy, A.; Gollihar, J. D.; Nourani, A.; Li, B.; Ellington, A. D. *Angew. Chem. Int. Ed.* **2017**, *56*, 992-996.

(20) Phillips, E. A.; Moehling, T. J.; Bhadra, S.; Ellington, A. D.; Linnes, J. C. *Anal. Chem.* **2018**, *90*, 6580-6586.

(21) Hu, J.; Jiang, Y.; Wu, L.; Wu, Z.; Bi, Y.; Wong, G.; Qiu, X.; Chen, J.; Pang, D.; Zhang, Z. *Anal. Chem.* **2017**, *89*, 13105-13111.

(22) Qin, C.; Wen, W.; Zhang, X.; Gu, H.; Wang, S. *Chem. Commun.* **2015**, *51*, 8273-8275.

(23) Chen, J.; Zhou, S.; Wen, J. *Anal. Chem.* **2014**, *86*, 3108-3114.

(24) Chen, J.; Zhou, X.; Zeng, L. *Chem. Commun.* **2013**, *49*, 984-986.

(25) Qin, C.; Gao, Y.; Wen, W.; Zhang, X.; Wang, S. *Biosens. Bioelectron.* **2016**, *79*, 522-530.

(26) Chen, J.; Fang, Z.; Lie, P.; Zeng, L. *Anal. Chem.* **2012**, *84*, 6321-6325.

(27) Li, J.; Macdonald, J. *Lab. Chip* **2016**, *16*, 242-245.

(28) Huang, Y.; Wen, W.; Du, D.; Zhang, X.; Wang, S.; Lin, Y. *Biosens. Bioelectron.* **2014**, *61*, 598-604.

(29) Nikitin, M. P.; Shipunova, V. O.; Deyev, S. M.; Nikitin, P. I. *Nature Nanotechnol.* **2014**, *9*, 716-722.

(30) Seelig, G.; Soloveichik, D.; Zhang, D. Y.; Winfree, E. *Science* **2006**, *314*, 1585-1588.

(31) Qian, L.; Winfree, E. *Science* **2011**, *332*, 1196-1201.

(32) Qian, L.; Winfree, E.; Bruck, J. *Nature* **2011**, *475*, 368-372.

(33) Elbaz, J.; Lioubashevski, O.; Wang, F.; Remacle, F.; Levine, R. D.; Willner, I. *Nature Nanotechnol.* **2010**, *5*, 417-422.

(34) Orbach, R.; Willner, B.; Willner, I. *Chem. Commun.* **2015**, *51*, 4144-4160.

(35) Yang, C.; Hsu, C.; Chuang, Y. *Chem. Commun.* **2012**, *48*, 112-114.

(36) Li, H.; Guo, S.; Liu, Q.; Qin, L.; Dong, S.; Liu, Y.; Wang, E. *Adv. Sci.* **2015**, *2*, 1500054.

(37) Xu, S.; Li, H.; Miao, Y.; Liu, Y.; Wang, E. *NPG Asia Mater.* **2013**, *5*, e76.

(38) Fratto, B. E.; Lewer, J. M.; Katz, E. *ChemPhysChem* **2016**, *17*, 2210-2217.

(39) Wu, C.; Wang, K.; Fan, D.; Zhou, C.; Liu, Y.; Wang, E. *Chem. Commun.* **2015**, *51*, 15940-15943.

(40) Li, H.; Liu, Y.; Dong, S.; Wang, E. *NPG Asia Mater.* **2015**, *7*, e166.

(41) Liu, S.; Li, M.; Yu, X.; Li, C.; Liu, H. *Chem. Commun.* **2015**, *51*, 13185-13188.

(42) Orbach, R.; Remacle, F.; Levine, R. D.; Willner, I. *Chem. Sci.* **2014**, *5*, 1074-1081.

(43) Jiang, X.; Ng, D. K. P. *Angew. Chem. Int. Ed.* **2014**, *53*, 10481-10484.

(44) Lu, J. Y.; Zhang, X. X.; Huang, W. T.; Zhu, Q. Y.; Ding, X. Z.; Xia, L. Q.; Luo, H. Q.; Li, N. B. *Anal. Chem.* **2017**, *89*, 9734-9741.

for TOC only

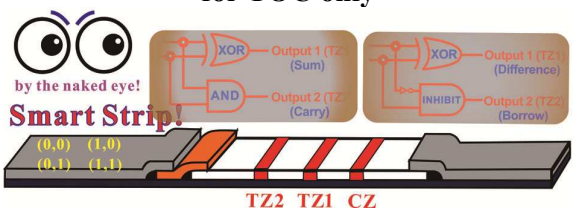
by the naked eye!
Smart Strip!
(0,0) (1,0)
(0,1) (1,1)
XOR
Output 1 (TZ
(Sum)
AND
Output 2 (TZ
(Carry)
XOR
Output 1 (TZ1)
(Difference)
INHIBIT
Output 2 (TZ2)
(Borrow)
TZ2 TZ1 CZ